Proceedings of GPPS Forum 18
Global Power and Propulsion Society
Zurich, 10th-12th January 2018
www.gpps.global

GPPS-2018-0024

SHAPE OPTIMIZATION IN LOW-ORDER THERMOACOUSTIC NETWORKS

José G. Aguilar
University of Cambridge
Department of Engineering
jga28@cam.ac.uk
Cambridge, United Kingdom

Matthew P. Juniper
University of Cambridge
Department of Engineering
mpj1001@cam.ac.uk
Cambridge, United Kingdom

ABSTRACT

Thermoacoustic oscillations arise due to the coupling between the acoustic field and the fluctuating heat release in a combustion chamber. In devices in which safety is paramount, such as aircraft engines, thermoacoustic oscillations must be eliminated passively, rather than through feedback control. The ideal way to eliminate them is by changing the shape of the device. To achieve this, one must calculate the sensitivity of each unstable thermoacoustic mode to every geometric parameter. This is prohibitively expensive with standard methods, but is relatively cheap with adjoint methods. In this paper we first present low-order network models as a tool to model and study the thermoacoustic behaviour of combustion chambers. Then we compute the continuous adjoint equations and the sensitivities to relevant parameters. With this, we run an optimization routine that modifies the parameters in order to stabilize all the resonant modes.

INTRODUCTION

Thermoacoustic oscillations are a form of combustion instabilities that may arise during the development of combustion systems such as jet engines or gas turbines. These instabilities appear due to the interaction between the flow field and the unsteady heat release process and manifest as large amplitude oscillations. If the instabilities grow they can produce noise, undesired vibrations and structural damage (Lieuwen and Yang, 2005). Hence, thermoacoustic oscillations impact the design of combustion systems.

Before the advent of analytical design tools, combustion instabilities had to be mitigated via passive control techniques or through an iterative empirical approach. Passive control methods include damping devices such as Helmholtz resonators or acoustic liners, which take advantage of thermo-viscous losses and vortex shedding to stabilize the system. However, these devices have the disadvantage of being effective only over a narrow frequency range and being unable to respond to changes in operating conditions. On the other hand, trial and error techniques are often exploited until a stable configuration is achieved. An example in jet engines is presented in Mongia et al. (2003) where they review a case in which several approaches to fix the instability were used, such as alternate fuelling modes, Helmholtz resonators, spray angle changes and fuel nozzle cavity fill and seal. Another example are the multiple full scale tests performed on the F-1 engines to find a stable configuration for the baffles in the injectors of the rocket engine (Oefelein and Yang, 1993). From these examples it is clear that this method, although effective, is prohibitively expensive and thus discouraged for practical industrial applications.

During the last decades several methods to predict and control combustion instabilities have been developed. These allow for more complex active and passive control systems. Active feedback control techniques (Dowling and Morgans, 2005) are able to adjust to the changing operating conditions but rely on the capabilities of the sensors and actuators. Novel hybrid control techniques, which consider variations in the geometry profile to stabilize a thermoacoustic system, have been considered in Zhao and Morgans (2009) and Zhao et al. (2011). In the first of these studies, Helmholtz resonators are tuned by varying the neck areas in order to stabilize the resonant modes in a Rijke tube. In the second, tuning of acoustic liners was performed by varying the pipe length and the bias flow rate. The major advantage of these techniques was that a broader frequency range can be covered.

Although active and passive control methods have proven to be effective at stabilizing thermoacoustic systems, these techniques require the addition of controlling devices, which adds complexity and failure modes. In devices in which safety is the primary concern, the ideal way to stabilize the system is to generate a configuration that is, in principle, not prone to these instabilities. Therefore, we are interested in developing an automated shape modification routine that is capable of producing a configuration that is stable to all modes within a given frequency range. The major advantage is that the frequency range can be as wide as the capability that the model has to accurately capture the physics of the problem. To produce this optimization algorithm we require a modelling approach, sensitivity analysis and an optimization routine.

To model a combustor, a common approach is to use low-order models. The approach used in this paper is similar to the thermoacoustic network model developed by Stow and Dowling (2001) and extended in Dowling and Stow (2003). Such models comprise a network of acoustic elements that allow the propagation of acoustic and convective waves which are connected by jump relations that enforce conservation of mass momentum and energy. To extract the gradient information of the system we use adjoint based sensitivity analysis. In thermoacoustics, Magri and Juniper (2013) applied eigenvalue sensitivity analysis using Galerkin methods and Aguilar et al. (2017) using wave based methods. In these papers they assess how resonant modes change when any of the parameters of the system are varied. Some of the outcomes were experimentally validated in Rigas et al. (2016); Jamieson et al. (2017); Jamieson and Juniper (2017). Once the direction in which the eigenvalues move is known, an optimization routine is required to compute the optimal variations in the parameters that will stabilize the configuration.

In this paper, we first introduce the low-order modelling approach of the thermoacoustic problem. Then we briefly go through the derivation of the adjoint equations and, with these, perform sensitivity analysis on the geometric parameters. With the above information we develop an optimization routine that stabilizes a combustor rig by modifying its shape.

METHODOLOGY

Low order network modelling

The main elements of a network model are the straight ducts, characterised by having cross sectional area A and length L. They are governed by the one dimensional Euler equations:

$$\frac{\partial \rho}{\partial t} + \rho \frac{\partial u}{\partial x} + u \frac{\partial \rho}{\partial x} = 0, \tag{1a}$$

$$\rho \frac{\partial u}{\partial t} + \rho u \frac{\partial u}{\partial x} + \frac{\partial p}{\partial x} = 0, \tag{1b}$$

$$\frac{\partial p}{\partial t} + u \frac{\partial p}{\partial x} + \gamma p \frac{\partial u}{\partial x} = 0, \tag{1c}$$

where ρ is the density, p is the pressure, u is the axial velocity, and γ is the ratio of heat capacities, which is assumed to be constant. Following the formalism developed by Stow and Dowling (2001), we linearise the equations by assuming that small perturbations propagate through a homogeneous base flow in the entire duct. The flow variables become $p = \bar{p}(x) + p'(x,t)$, etc. By considering flow perturbations with complex frequency ω the fluctuating variables turn into: $p'(x,t) = \hat{p}(x)\mathrm{e}^{i\omega t}$. The resultant governing equations form a wave equation whose solutions are travelling waves: two acoustic waves (A_+ and A_-) that propagate with speeds $\bar{c} \pm \bar{u}$ (where $\bar{c}$ is the mean speed of sound) and a convective wave (A_E) that propagates at the mean flow speed ($\bar{u}$).

To connect the ducts and allow the base flow and the travelling waves to propagate through the entire system, we consider modules of area increase, area decrease and heat sources. The modules of area increase assume that mass and energy fluxes are conserved, and the axial momentum is increased by the force exerted by the walls. Modules of area decrease assume conservation of mass flux, entropy and energy flux. Finally, the heat source module considers the kinematic balance of the source (i.e., Bloxsidge et al. (1988)) and assumes conservation of mass and momentum flux with an energy increase by the heat release. This module includes the unsteady heat release model, which is a velocity driven $n - \tau$ model:

$$\frac{\hat{Q}}{\bar{Q}} = n \frac{\hat{u}_1}{\bar{u}_1} \mathrm{e}^{-i\omega\tau} \tag{2}$$

Where Q is the heat release, n the interaction index and τ the time delay. We have also used subscript 1 to denote that the heat release model is proportional to the values just upstream of the heat source.

To fully characterize the system, we require inlet and outlet boundary conditions. The system can be modelled using open ends ($\hat{p} = 0$), closed ends ($\hat{u} = 0$), choked ends and reflection coefficients (R_c). The reflection coefficients are particularly interesting because they allow the model to use complex valued impedances as boundaries and are given by: $A_+ = R_c A_-$ at the inlet and $A_- \mathrm{e}^{ik_- x_0} = R_c A_+ \mathrm{e}^{ik_- x_0}$ at the outlet, where $k_\pm$ are the wave numbers and x_0 is the coordinate of the outlet boundary.

Using the different modules described above, we can build a network model that resembles a combustor. To solve for the eigenvalues of the system, we guess ω and, starting from the inlet boundary condition, we propagate the solution through each module until we reach the outlet boundary condition. In general, this condition will not be satisfied. Hence we create an iterative shooting method until the boundary condition is satisfied. The value of ω is then an eigenvalue, because it satisfies the governing equations and boundary conditions.

The adjoint equations

To obtain the adjoint equations used for the sensitivity analysis we first create a Lagrangian functional. Considering that $[\cdot,\cdot]$ is an appropriate inner product, the functional in its more general form is given by:

$$\mathscr{L} \equiv \omega - \left[\hat{q}^+, P(\omega, \hat{q}, G)\right] - \left[G^+, B(G)\right], \tag{3}$$

where ω is the eigenvalue of interest. $\hat{q}^{+}$ is the vector of Lagrange multipliers associated with P, which is the vector of perturbation equations, jump conditions, and boundary conditions that depend on the eigenvalue ω, the perturbation variables $\hat{q}$ and the base flow variables G. G^{+} is another vector of Lagrange multipliers associated to B, which is the vector of base flow equations, jump conditions and boundary conditions that depend on the base flow variables G.

Following the continuous adjoint method developed in Aguilar et al. (2017) we use the first inner product in Eq. (3) to compute the adjoint perturbation equations for the ducts, the adjoint jump conditions for each of the area increase, area decrease and heat source modules and the associated inlet and outlet adjoint boundary conditions. We note that changing a parameter such as the area induces base flow variations. Therefore, when computing the sensitivities we need to account for the changes generated in the perturbation equations and in the base flow. To compute the latter we require the knowledge of the adjoint base flow equations which are computed using the second inner product in the Lagrangian functional and following the procedure presented in Marquet et al. (2008).

Sensitivity analysis

In this study we are interested in knowing the eigenvalue drift whenever we make a small change in any of the geometric or heat source parameters. To compute the sensitivities we follow the methodology presented in Aguilar et al. (2017), which requires the knowledge of both the direct and the adjoint variables. Then, vanishing the derivative of the Lagrangian functional Eq. (3) with respect to the desired base state variable gives the sensitivity of the variable with respect to the eigenvalue. In this paper, the relevant base state variables are the area and length of the ducts, and the time-delay of the heat source.

Optimization

With the adjoint based sensitivity information, we can implement an optimization routine that resembles a gradient descent method. In this study we are interested in producing a configuration which stabilizes all of the unstable resonant modes of a thermoacoustic system. Hence, the following optimization routine is executed:

1. Compute the resonant modes of the system.
2. Compute sensitivity of the eigenvalues with respect to the relevant parameters: A, L, τ.
3. Given a set of constraints in the system, the sensitivities, and a maximum allowed change in the parameters, compute, by means of an optimization algorithm, the changes in the configuration, such that the new configuration evolves according to the cost function.
4. Update the configuration and iterate the process until all of the resonant modes are stabilized.

The cost function: by introducing a small change in one of the system's parameters (denoted by δx), the eigenvalues shift. The predicted eigenvalue Ω_j is given by: $\Omega_j = \omega_j + \delta\omega_j$, where ω_j is a resonant mode of the system, and $\delta\omega_j$ is the corresponding eigenvalue drift, which is given by:

$$\delta\omega_j = \sum_{k=1}^{N_x} \frac{\partial \omega_j}{\partial x_k}\delta x_k, \tag{4}$$

where N_x is the number of relevant parameters in the system. In the studied frequency range the system will have N_ω resonant modes, each of them represented by: $\omega_j = \sigma_j - i\lambda_j$ where σ is the angular frequency and λ is the growth rate. Our objective is to stabilize all of the resonant modes (i.e., $\lambda_j < 0$ for j = $1, ..., N_\omega$) by introducing small changes into the system. To ensure that all the modes are stabilized we set an objective growth rate λ_o such that $\lambda_o \leq 0$. Once a mode reaches this objective we will not seek to stabilize it any more. With this information we build a predictor function $\Psi_j(\delta x)$. This function gives 0 if a mode is or becomes stable or the growth rate plus the shift if it is unstable:

$$\Psi_j(\delta x) = \begin{cases} \Phi_j(\delta x) & \text{if } \Phi_j(\delta x) > 0, \\ 0 & \text{if } \Phi_j(\delta x) < 0, \end{cases}$$

$$\Phi_j(\delta x) = \underbrace{\lambda_j + \sum_{k=1}^{N_x} \frac{\partial \lambda_j}{\partial x_k}\delta x_k}_{-\mathrm{Im}\left\{\Omega_j(\delta x)\right\}} - \lambda_o.$$

The reduced version of the cost function $\mathscr{J}(\delta x)$, which we minimize, is then given by the sum of the predictor functions over all of the eigenvalues of the system.

By setting the objective growth rate to be $\lambda_0 \leq -1$ we can further add a small constraint to the cost function in order to select the parameters that produce the smallest variations in the configuration. By considering δx_{m_k}, the maximum allowed change of the kth parameter the cost function becomes:

$$\underbrace{\mathscr{J}(\delta x) = \sum_{j}^{N_\omega} \Psi_j(\delta x)}_{\text{Reduced version}} + \frac{1}{N_x}\sum_{k=1}^{N_X} \frac{|\delta x_k|}{\delta x_{m_k}}. \tag{5}$$

Whenever all the modes are stable, the first summation in the cost function is zero so the algorithm seeks the configuration that requires the smallest change.

Maximum allowed change: the maximum allowed change of a parameter in the system is set as the largest increase in its magnitude (given as a percentage of its original magnitude) before the Taylor test[1] fails due to higher order effects appearing in the finite difference computation.

Optimization algorithm: the optimization routine resembles a gradient descent method, where the cost function

[1]The Taylor test compares the eigenvalue drift calculated with the adjoint method ($\delta\omega_A$) against the one computed via a finite difference ($\delta\omega_F$). Given a small change in a parameter (δx), the difference between eigenvalue drifts ($|\delta\omega_F - \delta\omega_A|$) grows linearly with the square of the small change (δx^2).

is the sum of the growth rates of the unstable eigenvalues and the gradient is given by the sensitivities. Hence the easiest option to compute the values of δx would be to perform a line search. However, given the behaviour of the cost function Eq. (5), together with the upper and lower bounds given by the maximum allowed change, it is better to use an interior point method to look for the optimal values of δx. The constrained minimization problem which is to be solved using a barrier method is:

$$\begin{aligned} &\text{minimize} && \mathscr{J}(\delta x) \\ &\text{subject to} && -\delta x_{m_k} \leq \delta x_k \leq \delta x_{m_k}, \qquad k = 1, ..., N_x \end{aligned}$$

APPLICATION: Rama Balachandra's burner

Rama Balachandra's burner is a 10 kW combustor rig built in CUED, originally intended for the experimental investigation of the response of turbulent premixed flames to acoustic oscillations (Balachandran, 2005). One of the experimental cases focuses on a configuration with no swirl and imperfectly premixed combustion prone to self-excited oscillations. The geometry consists of an inlet duct connected to a plenum with a varying cross section at both ends, followed by the middle concentric ducts which contain the fuel injection plane and a centred bluff body which becomes the flame holder and finally a cylindrical pipe enclosure. The configuration is shown in Fig. 1.

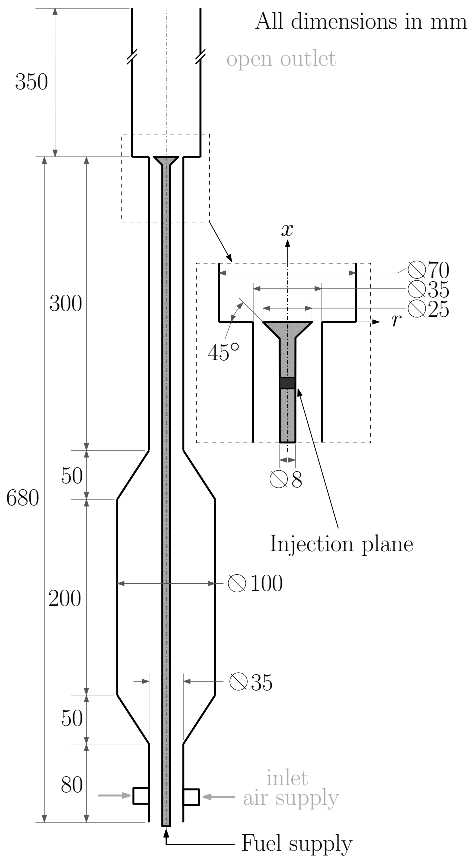

FIGURE 1: Schematic of Rama Balachandra's combustor rig.

Model inputs

Network model: to model the rig using the network model, we consider a total of 124 straight ducts. The varying cross sections of the plenum are modelled as a sequence of 50 area increase steps and 50 area decrease steps. To model the bluff body we further consider 20 area decrease steps.

Steady flow inputs: we consider air properties and constant specific heat capacities. At the inlet we consider atmospheric conditions and assume that air is supplied with a velocity of $\bar{u} = 5.16$ m/s to match the experimental measurement at the bluff body of $\bar{u} = 9.90$ m/s (Balachandran, 2005). We consider an open outlet and a flame anchored to the bluff body that supplies the system a steady heat input of $\bar{Q}_c = 5.00$ kW.

Fluctuating flow inputs: for the boundary conditions we consider an inlet modelled by an acoustic reflection coefficient with $R_c = 0.85 + 10i$, which resembles an almost closed end. The outlet is modelled with a frequency-dependent reflection coefficient of a circular duct radiating sound, originally proposed by Levine and Schwinger (1948). We will use the version that considers a mean flow proposed by Peters et al. (1993). Taking r as the duct radius, the reflection coefficient gives:

$$R_c = -\left(1 + \bar{M}A(St)\right)\left(1 - \frac{1}{2}\left(\frac{\omega r}{\bar{c}}\right)^2\right)\mathrm{e}^{i(k_+ - k_-)\delta(St)}, \quad (6)$$

where $\bar{M} = \bar{u}/\bar{c}$ is the Mach number, $St = \mathrm{Re}\{\omega\}r/(2\pi\bar{u})$ is the Strouhal number, $A(St)$ is a mean flow correction and $\delta(St)$ is the end correction. The last two are functions that depend on the Strouhal number only. In the cases that we will be exploring the Mach number is small and the frequencies big enough to consider the limiting behaviour of these quantities which are $A(St) = 0.90$ for $St \to \infty$ and $\delta(St) = 0.6133r$ for $\bar{M} \to 0$ and $St \to \infty$.

For the heat source, we will explore a velocity driven kinematic flame, with interaction index $n = 3.33$ and time delay $\tau = 8.4 \times 10^{-3}$s, which approximately matches the experimental results reported in (Balachandran, 2005).

The resonant modes

For frequencies up to 1000 Hz, Fig. 2 shows the logarithmic boundary condition error at the outlet for Rama Balachandran's rig. For the kinematic flame we observe that there are 7 unstable modes at 61, 162, 346, 433, 530, 621 and 736 Hz (where the boundary error is minimal). We observe that there is an unstable resonant mode near 348 Hz, which is the reported frequency for the self-excited combustor in the experimental investigation of Balachandran (2005).

Sensitivity analysis

The sensitivity analysis will be performed in every iteration of the optimization routine. In Fig. 3 we present the results for the initial configuration to analyse the initial trajectories of the changes in the geometry. The first observation

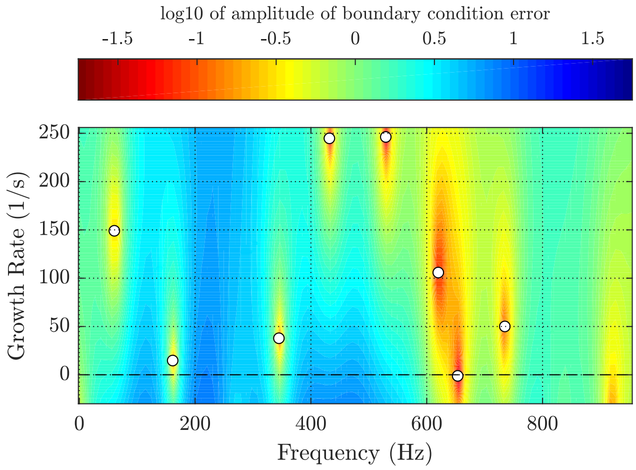

FIGURE 2: Logarithmic boundary condition error plot for the initial configuration of Rama's burner. The white markers denote the resonant modes found with the shooting method. Only resonant modes with growth rate $\lambda > -30$ s^{-1} are considered in this plot.

is that length sensitivities are one order of magnitude smaller than area sensitivities. The former can be explained given that a change in area causes base flow variations while a change in length does not. Hence, for area changes, the base flow sensitivity adds on to the unsteady sensitivity. In terms of sensitivity to changes in length, we observe that the plenum is close to the negative extreme so we expect an increase in length in the first iterations. The concentric ducts in the middle and the combustion chamber are close to the positive extreme, thus we expect them to shrink. We note that the sensitivity to changes in area of the inlet duct lies on the negative extreme, thus an increase in size is expected. The concentric ducts in the middle are close to the positive extreme hence we anticipate a reduction in area. Finally, the sensitivity of the area at the flame holder position is close to the negative extreme, so an area increase is likely in this region. In terms of time delay sensitivity we observe that it is an order of magnitude bigger than the area sensitivity, but there is no general trend for the growth rate shift. Therefore, to stabilize the system, we expect minor changes in this parameter.

Shape modification for stability

To run the optimization routine, we first identify the parameters that can be modified and then the constraints of the system, since these will determine the evolution of the configuration. Geometric parameters such as areas and lengths can be changed. The time delay in the unsteady heat release can also be changed, given that it is often related to the convection time of the fuel from the injection point until it reaches the flame (Dowling and Stow, 2003) and thus is determined by the geometry and the flow speeds. In summary, we define the following constrained cases:

- Case 1: Every module in the network is allowed to change only their area.
- Case 2: Every module in the network is allowed to change their length and area.
- Case 3: Every module in the network is allowed to change their length and area. The time delay in the flame parameters is also allowed to change.

We also keep a linear radius variation in the varying cross sections of the plenum and the bluff body.

Before starting the optimization routine, each of the sensitivities is checked with a Taylor test to ensure that they are correctly computed and to obtain the maximum allowed change. The maximum change was set to 1% of the current magnitude of the lengths and areas and 0.1% of the time delay. The cost function is given by Eq. (5). The objective growth rate is taken as $\lambda_o = -5/\text{s}$.

RESULTS

Figs. 4 and 5 show the initial and final configurations and spectrum for the burner with a kinematic flame after allowing the parameters to change according to the optimization routine until all of the resonant modes in the studied regime are stabilized.

Case 1: *Areas only*. From Fig. 4a we observe that the inlet duct, plenum and combustion chamber increased area, while the concentric ducts in the middle decreased area. The bluff body area reduction region changed to a region of area increase, the ratio of the area of the flame holder with respect to its original value is: 169%.

Case 2: *Lengths and areas*. From Fig. 4b we observe that the inlet duct and the combustion chamber gained volume, while the plenum and the concentric ducts in the middle lost volume. The area of the flame holder increased 178% with respect to its original value.

Case 3: *Lengths, areas and time delay*. From Fig. 4c we observe a similar evolution as in the previous case but the combustion chamber is longer. The time delay variation is 2.1% with respect to the original value.

DISCUSSION

From the boundary error plot in Fig. 2 it is clear that the thermoacoustic system is very unstable due to the amount of unstable eigenvalues, and also due to the magnitude of the growth rates. The consequence of this behaviour are the big changes required in the configuration to achieve full stability, which is observed in Fig. 4.

Some tendencies in the changes of the geometric parameters present in all cases are that: the inlet duct area increases, the middle concentric ducts area decreases, the combustion chamber gains volume, and the flame holder area increases. Most are predicted from the sensitivity analysis performed in the initial configuration of the rig. We further note that the change in the time delay is small. This is explained by the fact that the cost function is the sum of growth rates from many unstable eigenvalues. The direction of the growth rate shift is different for each eigenvalue and the influence of the time delay on the sum of these seems to be small.

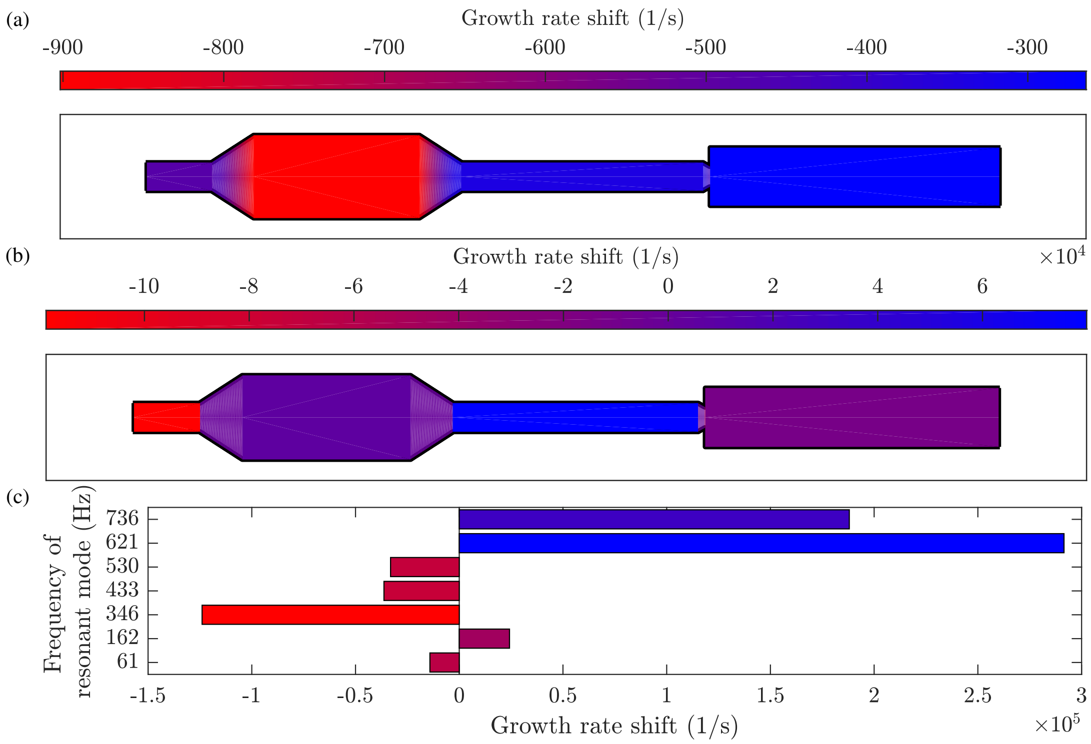

FIGURE 3: Sensitivity maps for the unstable modes in the initial configuration of Rama Balachandra's burner. (a) and (b) map the average growth rate shift due to changes in lengths and areas respectively. (c) shows the growth rate shift due to variations in the time delay of the unsteady heat release for every unstable resonant mode.

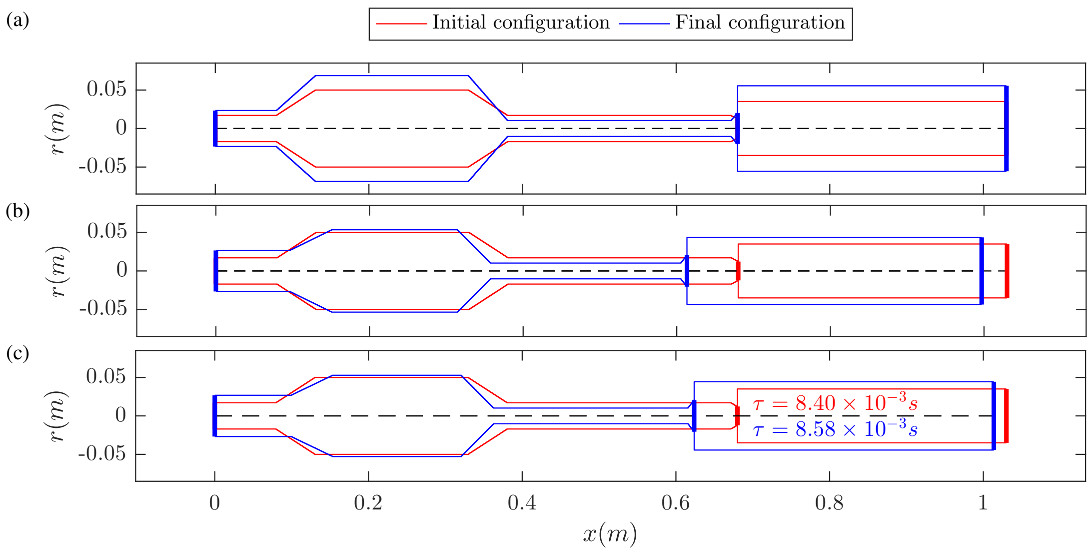

FIGURE 4: Initial (red) and final (blue) configurations for Rama's burner with a kinematic flame after all the resonant modes have been stabilized. (a), (b) and (c) show the configurations for variations in areas (Case 1), lengths and areas (Case 2) and lengths, areas and time delay (Case 3), respectively.

It is worth mentioning that during every iteration of the optimization routines, the most expensive computation is the calculation of the resonant modes. Solving for the adjoint variables, performing sensitivity analysis and running the optimization routine, account only for an additional computation each.

CONCLUSIONS

The main goal of this paper is to passively stabilize a model of a thermoacoustic rig by changing the geometric or heat source parameters using an adjoint-based optimization routine. First, we present the low-order model used to capture the physics of the system. Then we show how to obtain the adjoint equations and perform the sensitivity analysis. Then we

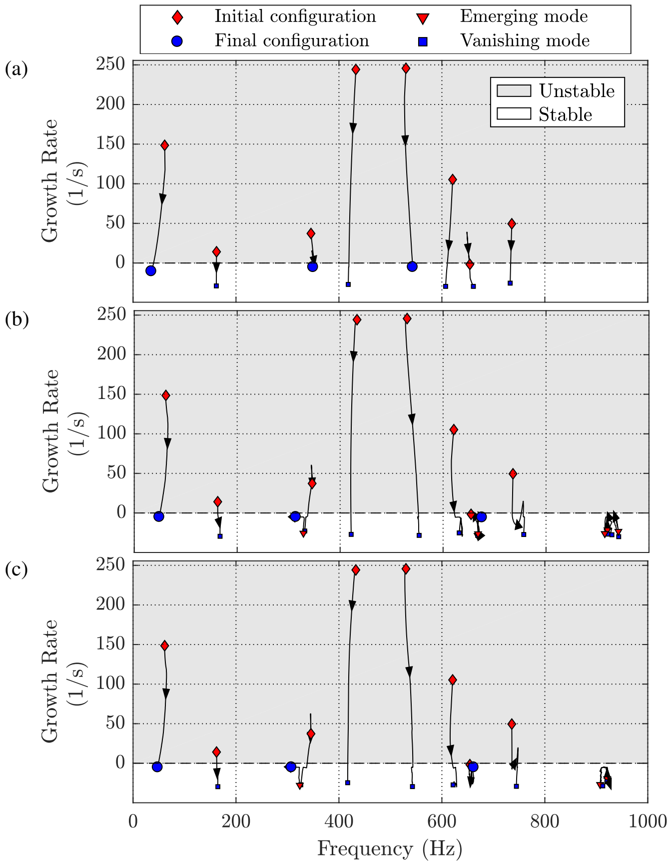

FIGURE 5: Eigenvalue trajectories from the initial (unstable) to the final (stable) configuration. The initial and final configurations are represented by the diamonds and circles respectively. Modes that emerge or vanish during the evolution of the configuration are represented by the triangles and squares respectively. (a), (b) and (c) show the spectrum for variations in areas (Case 1), lengths and areas (Case 2) and lengths, areas and time delay (Case 3), respectively. Only resonant modes with growth rate $\lambda > -30\ \mathrm{s}^{-1}$ are considered in these plots.

describe the optimization routine used to stabilize all the resonant modes of the system. Finally we apply this methodology to a model of a laboratory-scale rig in order to stabilize all of the resonant modes by changing the geometric and heat source parameters.

We show that the adjoint equations efficiently extract the gradients of the eigenvalues with respect to all parameters of the model. Initially, there are several unstable eigenvalues, and others become unstable during the optimization process. The cost function used in the optimization routine accounts for this and manages to stabilize all the eigenvalues of the burner. For this burner, it does so by making the inlet ducts, flame holder, and combustion chamber larger, while making the middle ducts smaller. This is not necessarily the only way to stabilize all the modes; it is likely that other configurations could be found with different starting conditions and optimization procedures.

The adjoint-based optimization routine in this paper could be used in the design phase to adjust the shape of a device in order to avoid thermoacoustic instability across multiple possible modes. It requires shape modifications, rather than the addition of devices such as Helmholtz resonators or acoustic liners. In industry, the cost function would need to be combined with practical constraints, but this should be relatively straight-forward. This method could be applied to larger and more complicated models. Thermoacoustic systems are, however, notoriously sensitive to small changes in some parameters. Therefore, although this method will work in general, the results will be quite specific to each configuration. Further, the results are only as good as the underlying thermoacoustic model.

The next stage of the research is to extend this approach to two dimensional configurations such as annular combustors. This will enable us to study the impact of circumferential and plane waves in the evolution of the geometric profiles.

Acknowledgements

José G. Aguilar gratefully acknowledges the financial support from CONACyT and The Cambridge Trust for funding this research.

REFERENCES

Aguilar, J. G., Magri, L. and Juniper, M. P. (2017), ‘Adjoint-based sensitivity analysis of low-order thermoacoustic networks using a wave-based approach’, *Journal of Computational Physics* **341**, 163–181.

Balachandran, R. (2005), Experimental Investigation of the Response of Turbulent Premixed Flames to Acoustic Oscillations, PhD thesis.

Bloxsidge, G. J., Dowling, A. P. and Langhorne, P. J. (1988), ‘Reheat buzz: an acoustically coupled combustion instability. Part 2. Theory’, *Journal of Fluid Mechanics* **193**, 445–473.

Dowling, A. P. and Morgans, A. S. (2005), ‘Feedback control of combustion oscillations’, *Annual Review of Fluid Mechanics* **37**(1), 151–182.

Dowling, A. P. and Stow, S. R. (2003), ‘Acoustic analysis of gas turbine combustors’, *Journal of Propulsion and Power* **19**(5), 751–764.

Jamieson, N. P. and Juniper, M. P. (2017), ‘Experimental Sensitivity Analysis and the Equivalence of Pulsed Forcing and Feedback Control in Thermoacoustic Systems’, *ASME Turbo Expo* pp. GT2017–63441.

Jamieson, N. P., Rigas, G. and Juniper, M. P. (2017), ‘Experimental sensitivity analysis via a secondary heat source in an oscillating thermoacoustic system’, *International Journal of Spray and Combustion Dynamics* **0**(0), 1–11.

Levine, H. and Schwinger, J. (1948), ‘On the radiation of sound from an unflanged circular pipe’, *Physical Review* **73**(4), 383–406.

Lieuwen, T. C. and Yang, V., eds (2005), *Combustion instabilities in gas turbine engines: operational experience, fundamental mechanisms, and modeling*, AIAA.

Magri, L. and Juniper, M. P. (2013), ‘Sensitivity analysis of a time-delayed thermo-acoustic system via an adjoint-based approach', *Journal of Fluid Mechanics* **719**, 183–202.

Marquet, O., Sipp, D. and Jacquin, L. (2008), 'Sensitivity analysis and passive control of cylinder flow', *Journal of Fluid Mechanics* **615**, 221–252.

Mongia, H. C., Held, T. J., Hsiao, G. C. and Pandalai, R. P. (2003), 'Challenges and progress in controlling dynamics in gas turbine combustors', *Journal of Propulsion and Power* **19**(5), 822–829.

Oefelein, J. C. and Yang, V. (1993), 'Comprehensive Review of Liquid-Propellant Combustion Instabilities in F-1 Engines', *Journal of Propulsion and Power* **9**(5), 657–677.

Peters, M. C. a. M., Hirschberg, a., Reijnen, a. J. and Wijnands, a. P. J. (1993), 'Damping and reflection coefficient measurements for an open pipe at low Mach and low Helmholtz numbers', *Journal of Fluid Mechanics* **256**(-1), 499.

Rigas, G., Jamieson, N. P., Li, L. K. B. and Juniper, M. P. (2016), 'Experimental sensitivity analysis and control of thermoacoustic systems', *Journal of Fluid Mechanics* **787**, R1 1–11.

Stow, S. R. and Dowling, A. P. (2001), 'Thermoacoustic oscillations in an annular combustor', *ASME Turbo Expo* pp. 2001–GT–0037.

Zhao, D. and Morgans, A. S. (2009), 'Tuned passive control of combustion instabilities using multiple Helmholtz resonators', *Journal of Sound and Vibration* **320**(4-5), 744–757.

Zhao, D., Morgans, A. S. and Dowling, A. P. (2011), 'Tuned Passive Control of Acoustic Damping of Perforated Liners', *AIAA Journal* **49**(4), 725–734.